Spectral Representation of Three-Dimensional Global Data by Expansion in Normal Mode Functions

AKIRA KASAHARA AND KAMAL PURI[1]

National Center for Atmospheric Research,[2] Boulder, CO 80307

(Manuscript received 8 January 1980, in final form 28 July 1980)

ABSTRACT

To represent atmospheric data spectrally in three indices (zonal wavenumber, and meridional and vertical modal indices), we propose to use three-dimensional normal mode functions (NMF's) to express the wind and mass fields simultaneously. The NMF's are constructed from the eigensolutions of a global primitive equation model and they are orthogonal functions. The vertical parts are obtained from the solutions of the vertical structure equation with the equivalent height as the eigenvalue. The vertical modal index is associated with a different value of the equivalent height. The horizontal parts of NMF's are Hough harmonics with zonal wavenumber and meridional modal index as two-dimensional scalings. The expansion of global data in terms of NMF's permits the partition of energy into two distinct kinds of motions—gravity-inertia modes and rotational modes of Rossby/Haurwitz type. Both kinds of motion are also partitioned into different vertical modes. Results of the spectral distribution of atmospheric energy, obtained by expanding in the NMF's hemispherical data of the National Meteorological Center, are presented. Information obtained will be useful to select proper horizontal and vertical computational resolutions for representation of atmospheric data.

1. Introduction

Information on the spectral distribution of atmospheric energy is important to proper selection of computational resolutions for solving prognostic equations. Such information is also useful in parameterizing subgrid-scale energy dissipation mechanisms in the prediction equations in either the finite-difference or spectral form. Most of the past studies on atmospheric energy spectra, for example, those summarized by Leith (1971), are those of kinetic energy in longitudinal scale based on Fourier expansions of data at various latitudes and pressure levels. In order to represent the spectral distributions of energy in latitudinal and longitudinal scales, one needs to utilize two-dimensional expansion functions to represent data. Because spherical harmonics are eigensolutions of the barotropic nondivergent vorticity equation over a sphere, they are suitable basis functions to represent atmospheric energetics in global scales (Baer, 1972; Burrows, 1976; Chen and Wiin-Nielsen, 1978). However, in these studies the vertical structures of statistics are presented spatially rather than spectrally with a suitable vertical scaling. It is desirable, then, to seek the spectral representation of three-dimensional data in which the vertical dependences are also decomposed spectrally.

Traditionally, the vertical structures of atmospheric data are represented by empirical orthogonal functions (EOF's) as described by Obukhov (1960) and Holmström (1963). The expansion of data in empirically-defined orthogonal functions is efficient, because the method minimizes the root-mean-square difference between the data and the functional representation. The physics of the atmosphere is reflected statistically in the characteristics of EOF's. With respect to the vertical structure of transient motions, there have been some attempts to interpret the physical characteristics of EOF's based on atmospheric equations (Holmström, 1964, and Gavrilin, 1965). Along the same vein, in an attempt to relate a vertical scaling with horizontal scalings Baer (1981) adopted eigensolutions of the vertical differential operator of a quasi-geostrophic potential vorticity equation to fit the structure of EOF's. The combination of spherical harmonic expansion in the horizontal and EOF expansion in the vertical has been used by Bradley and Wiin-Nielsen (1968) in an investigation of transient planetary wave structures.

One shortcoming in all of the previous studies is that scale information on atmospheric energies is derived separately from the wind field (velocity components) and the mass field (geopotential height or temperature) and it is often difficult to merge two informations together. Flattery (1970), however,

[1] Permanent affiliation: Australian Numerical Meteorology Research Centre, Melbourne, Victoria, Australia.

[2] The National Center for Atmospheric Research is sponsored by the National Science Foundation.

0027-0644/81/010037-15$07.75

developed an objective analysis procedure whereby the vertical structures of wind and geopotential height are represented by common EOF's and the horizontal structure is represented by the rotational parts of Hough harmonics corresponding to the external mode. Hough harmonics are the eigensolutions of linearized shallow-water equations over a sphere (Laplace tidal equations). Even in his approach, because of the absence of relationships between the expansion functions in the horizontal and vertical directions, it is not possible to map a complete spectral energy distribution in three-dimensional indices.

We propose in this paper an alternate approach—the use of three-dimensional normal mode functions (NMF's), which are completely orthogonal, to represent the velocity and mass simultaneously. NMF's are eigensolutions of a linearized primitive equation model.

The expansion of data in terms of three-dimensional NMF's was performed by V. Penenko, Siberian Branch of the Academy of Sciences of the USSR (private communication, 1976), Williamson and Dickinson (1976), Daley (1979), and Temperton and Williamson (1979). Penenko constructed NMF's by the finite-difference method based on a three-dimensional linearized primitive equation model in which the basic zonal flow, temperature and pressure are functions of height, latitude, and longitude. Williamson and Dickinson (1976) also constructed NMF's by the finite-difference method based on a three-dimensional linearized primitive equation model with a basic state at rest and the basic temperature and pressure profiles depending on height only. Temperton and Williamson (1979) applied the same technique to a linearized version of the European Centre for Medium Range Weather Forecasts (ECMWF) grid point forecast model. Their NMF's are not in general orthogonal in the vertical and, therefore, their expansions do not permit partition of the total energy in terms of each vertical mode separately. Daley (1979), on the other hand, formulated NMF's by the spectral method in the horizontal and the finite-element method in the vertical based on the Canadian operational primitive equation spectral model for application to nonlinear normal mode initialization.

In this paper, we present the construction of three-dimensional NMF's based on a linearized version of a global primitive equation model. The basic equations used are identical to those adopted by Daley (1979), but the selection of the variables to be expanded is made differently so that the orthogonality of the vertical structure functions is insured in the vertical structure functions themselves rather than their vertical derivatives.

In Section 2, we present the basic primitive equations in sigma coordinates with the upper and lower boundary conditions. In Section 3, a linearized version of the basic equations for a non-isothermal basic state at rest is discussed. In Section 4, solutions of the vertical structure equation with the arbitrary placement of vertical levels are presented. Section 5 contains a discussion of solutions of the horizontal structure equations. In Section 6, we demonstrate that the present discretization of vertical modes permits the partition of total energy into the kinetic and available potential energy of each vertical mode separately, and in Section 7, we discuss the expansion of three-dimensional global data in terms of the NMF's thus derived. Section 8 contains the results of the spectral distribution of atmospheric energy, obtained by expanding hemispherical data of the National Meteorological Center (NMC) in the NMF's in the framework of the Australian Numerical Meteorology Research Centre (ANMRC) spectral model (Bourke *et al.*, 1977). Conclusions are stated in Section 9.

2. Basic equations

We consider spherical coordinates in the horizontal with sigma coordinates in the vertical

$$\sigma = p/p_H, \tag{2.1}$$

where p and p_H denote the pressure and surface pressure, respectively.

The upper and lower boundary conditions utilized in our dynamical system are that

$$\dot{\sigma} = \frac{d\sigma}{dt} = 0 \quad \text{at} \quad \sigma = 0 \quad \text{and} \quad 1, \tag{2.2}$$

where $\dot{\sigma}$ is the vertical σ velocity and d/dt denotes the total derivative.

In spherical coordinates, the equations of horizontal motion, thermodynamics, surface pressure tendency, mass continuity and hydrostatic equilibrium for an adiabatic and inviscid atmosphere are given by (Robert *et al.*, 1972)

$$\frac{du}{dt} - \left(f + \frac{u \tan\phi}{a}\right)v = -\frac{1}{a\cos\phi}\left(g\frac{\partial z}{\partial\lambda} + RT\frac{\partial q}{\partial\lambda}\right), \tag{2.3}$$

$$\frac{dv}{dt} + \left(f + \frac{u \tan\phi}{a}\right)u = -\frac{1}{a}\left(g\frac{\partial z}{\partial\phi} + RT\frac{\partial q}{\partial\phi}\right), \tag{2.4}$$

$$\frac{dT}{dt} = \kappa T\left[\frac{\dot{\sigma}}{\sigma} - \nabla\cdot\tilde{\mathbf{V}} + (\mathbf{V} - \tilde{\mathbf{V}})\cdot\nabla q\right], \tag{2.5}$$

$$\frac{\partial q}{\partial t} + \tilde{\mathbf{V}}\cdot\nabla q + \nabla\cdot\tilde{\mathbf{V}} = 0, \tag{2.6}$$

$$\frac{\partial \dot{\sigma}}{\partial \sigma} + \nabla\cdot(\mathbf{V} - \tilde{\mathbf{V}}) + (\mathbf{V} - \tilde{\mathbf{V}})\cdot\nabla q = 0, \tag{2.7}$$

$$g\frac{\partial z}{\partial \sigma} = -\frac{RT}{\sigma}, \tag{2.8}$$

with the definitions

$$\frac{d}{dt} = \frac{\partial}{\partial t} + \mathbf{V}\cdot\nabla + \dot{\sigma}\frac{\partial}{\partial \sigma}, \tag{2.9}$$

$$\mathbf{V}\cdot\nabla = \frac{u}{a\cos\phi}\frac{\partial}{\partial \lambda} + \frac{v}{a}\frac{\partial}{\partial \phi}, \tag{2.10}$$

$$\nabla\cdot\mathbf{V} = \frac{1}{a\cos\phi}\left[\frac{\partial u}{\partial \lambda} + \frac{\partial}{\partial \phi}(v\cos\phi)\right], \tag{2.11}$$

$$q = \ln p_H, \tag{2.12}$$

where λ and ϕ are longitude and latitude, t time, $\mathbf{V} = (u,v)$ the horizontal velocity with u and v being the longitudinal and meridional components, z the geopotential height, T temperature, R gas constant, C_p specific heat at constant pressure, $\kappa = R/C_p$, g earth's gravity, a earth's radius, Ω earth's angular velocity of rotation, and f denotes $2\Omega\sin\phi$. Also,

$$\tilde{\mathbf{V}} = \int_0^1 \mathbf{V}\,d\sigma \tag{2.13}$$

is the vertically-averaged horizontal velocity.

We now introduce two new variables P and W defined by

$$\left.\begin{aligned} P &= gz + RT_0(\sigma)q \\ W &= \dot{\sigma} - \sigma(\nabla\cdot\tilde{\mathbf{V}} + \tilde{\mathbf{V}}\cdot\nabla q)\end{aligned}\right\}, \tag{2.14}$$

where $T_0(\sigma)$ is a mean temperature in the forecast domain and depends only on the vertical coordinate σ.

Using variable P, we rewrite the equations of horizontal motion (2.3) and (2.4) as

$$\frac{\partial u}{\partial t} - 2\Omega\sin\phi v + \frac{1}{a\cos\phi}\frac{\partial P}{\partial \lambda} = C_1, \tag{2.15}$$

$$\frac{\partial v}{\partial t} + 2\Omega\sin\phi u + \frac{1}{a}\frac{\partial P}{\partial \phi} = C_2, \tag{2.16}$$

where

$$\left.\begin{aligned} C_1 &= -\mathbf{V}\cdot\nabla u - \dot{\sigma}\frac{\partial u}{\partial \sigma} - \frac{RT'}{a\cos\phi}\frac{\partial q}{\partial \lambda} + \frac{uv\tan\phi}{a} \\ C_2 &= -\mathbf{V}\cdot\nabla v - \dot{\sigma}\frac{\partial v}{\partial \sigma} - \frac{RT'}{a}\frac{\partial q}{\partial \phi} - \frac{u^2\tan\phi}{a}\end{aligned}\right\}$$

and T' is the deviation of temperature T from the mean temperature $T_0(\sigma)$ so that

$$T' = T - T_0(\sigma). \tag{2.17}$$

Using variable W, we rewrite the continuity equation (2.7) as

$$\partial W/\partial \sigma + \nabla\cdot\mathbf{V} = -\mathbf{V}\cdot\nabla q. \tag{2.18}$$

We now need to express the thermodynamic equation (2.5) using variables P and W. By differentiating the definition of P in (2.14) with respect to σ and using the hydrostatic equation (2.8), we obtain

$$\frac{\partial P}{\partial \sigma} = -\frac{RT}{\sigma} + R\frac{dT_0}{d\sigma}q. \tag{2.19}$$

By differentiating the above equation with respect to t and utilizing (2.5), (2.6) and (2.14), we have, after some manipulation,

$$\frac{\sigma}{R\Gamma_0}\frac{\partial}{\partial t}\left(\frac{\partial P}{\partial \sigma}\right) + W = C_3, \tag{2.20}$$

where

$$C_3 = \frac{1}{\Gamma_0}\left(\mathbf{V}\cdot\nabla T' - \frac{\kappa T'}{\sigma}W + \dot{\sigma}\frac{\partial T'}{\partial \sigma} - \kappa T\mathbf{V}\cdot\nabla q\right)$$

and

$$\Gamma_0 = \frac{\kappa T_0}{\sigma} - \frac{dT_0}{d\sigma} \tag{2.21}$$

is a measure of the static stability of the basic atmosphere.

The boundary conditions for the original system are given by (2.2). In the new system with P and W, one of the boundary conditions becomes $W = 0$ at $\sigma = 0$ which is the consequence of $\dot{\sigma} = 0$ at $\sigma = 0$. The other condition can be derived from the surface pressure tendency equation (2.6) coupled with the definition of P and W at $\sigma = 1$. Consequently, the boundary conditions for the new system become

$$W = 0 \quad \text{at} \quad \sigma = 0, \tag{2.22}$$

$$\frac{\partial P_H}{\partial t} - RT_0W_H = 0 \quad \text{at} \quad \sigma = 1, \tag{2.23}$$

where P_H and W_H are defined by

$$\left.\begin{aligned} P_H &= gH + R(T_0)_H q, \\ W_H &= -(\nabla\cdot\tilde{\mathbf{V}} + \tilde{\mathbf{V}}\cdot\nabla q),\end{aligned}\right\} \tag{2.24}$$

in which $H(\lambda,\phi)$ denotes the elevation of the earth's surface and subscript H for P, W and T_0 refer to their surface values.

3. Linearized equations

We consider motions of small amplitude superimposed on a basic state at rest with temperature T_0 as a function of σ only. We denote perturbation

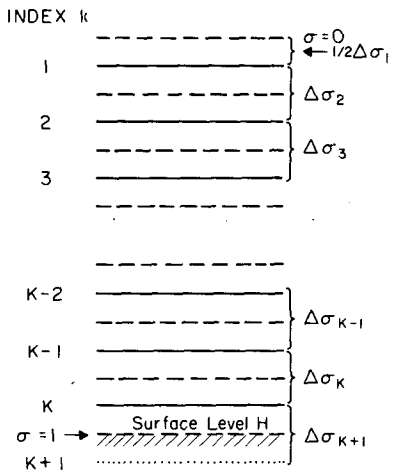

FIG. 1. Discrete representation of variables in the vertical. Solid lines show sigma levels at which (4.2) is solved.

variables by a prime. The right-hand sides of (2.15), (2.16), (2.18) and (2.20) represent nonlinear terms. By neglecting those right-hand side terms, we obtain the following system of linearized equations:

$$\frac{\partial u'}{\partial t} - 2\Omega v' \sin\phi = -\frac{\partial P'}{a\cos\phi\partial\lambda}, \tag{3.1}$$

$$\frac{\partial v'}{\partial t} + 2\Omega u' \sin\phi = -\frac{\partial P'}{a\partial\phi}, \tag{3.2}$$

$$\frac{\partial W'}{\partial\sigma} + \nabla\cdot\mathbf{V}' = 0, \tag{3.3}$$

$$\frac{\sigma}{R\Gamma_0}\frac{\partial}{\partial t}\left(\frac{\partial P'}{\partial\sigma}\right) + W' = 0. \tag{3.4}$$

Elimination of W' between (3.3) and (3.4) yields

$$\frac{\partial}{\partial t}\left[\frac{\partial}{\partial\sigma}\left(\frac{\sigma}{R\Gamma_0}\frac{\partial P'}{\partial\sigma}\right)\right] - \nabla\cdot\mathbf{V}' = 0. \tag{3.5}$$

Eqs. (3.1), (3.2), and (3.5) constitute a system of equations for u', v' and P'. The boundary conditions (2.22) and (2.23) imply

$$\frac{\partial P'}{\partial\sigma} = \text{finite} \quad \text{at} \quad \sigma = 0, \tag{3.6}$$

$$\frac{\partial P'}{\partial\sigma} + \frac{\Gamma_0}{T_0}P' = 0 \quad \text{at} \quad \sigma = 1. \tag{3.7}$$

The lower boundary condition (3.7) is derived by combining (2.23) and (3.4) and evaluating at $\sigma = 1$.

We now assume the following separation of variables by introducing a new vertical dependence function $\Psi(\sigma)$:

$$\left.\begin{aligned} u' &= \tilde{u}\Psi(\sigma) \\ v' &= \tilde{v}\Psi(\sigma) \\ P' &= g\tilde{h}\Psi(\sigma) \end{aligned}\right\}. \tag{3.8}$$

By substituting (3.8) into (3.1), (3.2) and (3.5), we find

$$\frac{\partial\tilde{u}}{\partial t} - 2\Omega\sin\phi\tilde{v} = -\frac{g}{a\cos\phi}\frac{\partial\tilde{h}}{\partial\lambda}, \tag{3.9}$$

$$\frac{\partial\tilde{v}}{\partial t} + 2\Omega\sin\phi\tilde{u} = -\frac{g}{a}\frac{\partial\tilde{h}}{\partial\phi}, \tag{3.10}$$

$$\frac{\partial\tilde{h}}{\partial t} + D\nabla\cdot\tilde{\mathbf{V}} = 0, \tag{3.11}$$

where the separation constant D with a dimension of height must satisfy the differential equation for $\Psi(\sigma)$:

$$\frac{d}{d\sigma}\left(\frac{\sigma g}{R\Gamma_0}\frac{d\Psi}{d\sigma}\right) + \frac{1}{D}\Psi = 0. \tag{3.12}$$

The boundary conditions (3.6) and (3.7) imply

$$\left.\begin{aligned} &\frac{d\Psi}{d\sigma} = \text{finite} \quad \text{at} \quad \sigma = 0 \\ &\frac{d\Psi}{d\sigma} + \frac{\Gamma_0}{T_0}\Psi = 0 \quad \text{at} \quad \sigma = 1 \end{aligned}\right\}. \tag{3.13}$$

The horizontal structures of solutions are determined from (3.9)–(3.11) once the value of separation constant D is found as an eigenvalue of the vertical structure equation (3.12) under boundary conditions (3.13). Since the horizontal structure equations (3.9)–(3.11) are identical to linearized equations of the shallow-water model with the height of fluid being D, we refer to D as equivalent height. Some aspects of the vertical structure equation (3.12) with boundary conditions (3.13) have been discussed by Wiin-Nielsen (1971).

4. Solutions of the vertical structure equation

The vertical structure equation (3.12) and boundary conditions (3.13) constitute a Sturm-Liouville problem. Consequently, it is straightforward to prove that the eigenfunctions Ψ_i and Ψ_j corresponding to eigenvalues D_i and D_j, when $D_i \neq D_j$, are orthogonal. Combination of its orthogonality with the normalization of the eigenfunctions yields

$$\int_0^1 \Psi_i(\sigma)\Psi_j(\sigma)d\sigma = \delta_{ij}, \tag{4.1}$$

where $\delta_{ij} = 1$ if $i = j$ and zero otherwise.

We rewrite (3.12) as

$$\frac{d}{d\sigma}\left(\beta\sigma\frac{d\Psi}{d\sigma}\right) + \lambda\Psi = 0, \tag{4.2}$$

where

$$\left.\begin{aligned} \beta &= gH_{00}/(R\Gamma_0) \\ \lambda &= H_{00}/D \end{aligned}\right\}, \tag{4.3}$$

in which H_{00} is a constant with a dimension of height. Since the equivalent height D appears as an eigen-

value, we use the symbol λ as a dimensionless eigenvalue. (There will be no confusion in the use of λ here even though it is used for longitude earlier.)

A discrete representation of data in the vertical is more common even for spectral models. Using the finite-difference method, we solve the vertical structure equation (4.2) for Ψ at sigma levels shown by solid lines in Fig. 1. The additional sigma level corresponding to $k = K + 1$ is created to handle the lower boundary condition. The ground level $\sigma = 1$ will be denoted by the subscript H.

The finite difference form of (4.2) may be given by

$$\frac{2}{(\Delta\sigma_1 + \Delta\sigma_2)}\left[(\sigma\beta)_{1\ 1/2}\frac{\Psi(2) - \Psi(1)}{\Delta\sigma_2} - 0\right] + \lambda\Psi(1) = 0,$$

$$\frac{2}{(\Delta\sigma_2 + \Delta\sigma_3)}\left[(\sigma\beta)_{2\ 1/2}\frac{\Psi(3) - \Psi(2)}{\Delta\sigma_3} - (\sigma\beta)_{1\ 1/2}\frac{\Psi(2) - \Psi(1)}{\Delta\sigma_2}\right] + \lambda\Psi(2) = 0,$$

— — —

— — —

— — —

$$\frac{2}{(\Delta\sigma_{K-1} + \Delta\sigma_K)}\left[(\sigma\beta)_{K-1/2}\frac{\Psi(K) - \Psi(K-1)}{\Delta\sigma_K} - (\sigma\beta)_{K-1\ 1/2}\frac{\Psi(K-1) - \Psi(K-2)}{\Delta\sigma_{K-1}}\right] + \lambda\Psi(K-1) = 0,$$

$$\frac{2}{(\Delta\sigma_K + \Delta\sigma_{K+1})}\left[(\sigma\beta)_H\frac{\Psi(K+1) - \Psi(K)}{\Delta\sigma_{K+1}} - (\sigma\beta)_{k-1/2}\frac{\Psi(K) - \Psi(K-1)}{\Delta\sigma_K}\right] + \lambda\Psi(K) = 0. \quad (4.4)$$

The upper boundary condition at $\sigma = 0$ is incorporated in the first equation as indicated by zero. Half integers are used to represent mid-levels of two consecutive sigma levels.

The lower boundary condition of (3.13) may be expressed in the form

$$\frac{\Psi(K+1) - \Psi(K)}{\Delta\sigma_{K+1}} = -\tfrac{1}{2}\hat{a}[\Psi(K+1) + \Psi(K)], \quad (4.5)$$

where

$$\hat{a} = (\Gamma_0/T_0)_H. \quad (4.6)$$

The unknown $\Psi(K+1)$ can be expressed in terms of $\Psi(K)$ through (4.5). When this is done, we obtain

$$\frac{\Psi(K+1) - \Psi(K)}{\Delta\sigma_{K+1}} = -\frac{b}{\Delta\sigma_{K+1}}\Psi(K), \quad (4.7)$$

where

$$b = \hat{a}\Delta\sigma_{K+1}/(1 + \tfrac{1}{2}\hat{a}\Delta\sigma_{K+1}). \quad (4.8)$$

By taking into account the lower boundary condition (4.7), we can prove from system (4.4) that the eigenfunctions $\Psi_i(k)$ and $\Psi_j(k)$ at sigma level k corresponding to eigenvalues λ_i and λ_j, when $\lambda_i \neq \lambda_j$, are orthogonal in the sense that

$$\sum_{k=1}^{K}\Psi_i(k)\Psi_j(k)\tfrac{1}{2}(\Delta\sigma_k + \Delta\sigma_{k+1}) = 0 \quad (4.9)$$

for $i \neq j$. This orthogonality condition suggests that the proper definition of the vertical structure function in the finite-difference framework is

$$\Phi(k) = \Psi(k)[\tfrac{1}{2}(\Delta\sigma_k + \Delta\sigma_{k+1})]^{1/2}. \quad (4.10)$$

With this definition of $\Phi(k)$, system (4.4) can be written in the matrix form

$$\mathbf{M}\Phi = \lambda\Phi,$$

where Φ is the eigenvector

$$\Phi = [\Phi(1), \Phi(2), \ldots, \Phi(K-1), \Phi(K)]^{\mathrm{T}} \quad (4.11)$$

and $\mathbf{M}$ is the matrix

$$\mathbf{M} = \begin{bmatrix} \frac{C_1}{d_1^2} & \frac{-C_1}{d_1d_2} & 0 & 0 & \cdots & 0 \\ \frac{-C_1}{d_1d_2} & \frac{(C_1 + C_2)}{d_2^2} & \frac{-C_2}{d_2d_3} & 0 & \cdots & 0 \\ \vdots & \frac{-C_{k-1}}{d_{k-1}d_k} & \frac{C_{k-1} + C_k}{d_k^2} & \frac{-C_k}{d_kd_{k+1}} & & \vdots \\ 0 & \cdots\ 0 & \frac{-C_{K-2}}{d_{K-2}d_{K-1}} & \frac{(C_{K-2} + C_{K-1})}{d_{K-1}^2} & & \frac{-C_{K-1}}{d_{K-1}d_K} \\ 0 & \cdots\ 0 & 0 & \frac{-C_{K-1}}{d_{K-1}d_K} & & \frac{(C_{K-1} + C_K)}{d_K^2} \end{bmatrix} \quad (4.12)$$

in which

$$\left.\begin{aligned} C_k &= \frac{(\sigma\beta)_{k+1/2}}{\Delta\sigma_{k+1}}, \qquad k = 1, 2, \ldots, K-1 \\ C_K &= \frac{\beta_H b}{\Delta\sigma_{K+1}} = \frac{\beta_H \hat{a}}{1 + 0.5\hat{a}\Delta\sigma_{K+1}} \\ &= \frac{gH_{00}}{R(T_0)_H(1 + 0.5\hat{a}\Delta\sigma_{K+1})} \\ d_k &= [0.5(\Delta\sigma_k + \Delta\sigma_{k+1})]^{1/2}, \qquad k = 1, 2, \ldots, K \end{aligned}\right\} . \tag{4.13}$$

Clearly, the matrix **M** is symmetric so that an eigenvalue λ and the associated eigenfunction are real. By combining with the normalization of eigenvectors, the orthogonality of Φ is expressed by

$$\sum_{k=1}^{K} \Phi_i(k)\Phi_j(k) = \delta_{ij}. \tag{4.14}$$

Since **M** of (4.12) is a symmetric matrix of order K, we obtain K eigenvalues λ and the associated eigenvectors Φ. With the scaling of H_{00} introduced in (4.3), the eigenvalue λ corresponds to the equivalent height D. Hence, we obtain K equivalent heights. The largest equivalent height (~10 km for the standard atmosphere) is referred to as the external mode. The rest of the equivalent heights correspond to internal modes. To show a specific example, an equivalent height D and the associated vertical structure function Φ are determined for the sigma system similar to that of the ANMRC spectral model (Bourke *et al.*, 1977) by solving matrix **M** of (4.12) constructed using nine sigma levels σ = 0.991, 0.926, 0.811, 0.664, 0.500, 0.336, 0.189, 0.074 and 0.009. The static stability distribution Γ_0 defined by (2.21) is calculated from the hemispherically-averaged monthly mean temperature $T_0(\sigma)$ of January 1977. The values of equivalent height thus obtained are found to be 9570, 3262, 817, 256, 105, 40, 23, 10 and 3 m. Fig. 2 shows the vertical distributions of eigenfunctions $\Phi_n(k)$ corresponding to equivalent heights D_n.

5. Solutions of the horizontal structure equations

Various aspects of the solutions of horizontal structure equations (3.9)–(3.11), which are often referred to as Laplace's tidal equations, are discussed by Longuet-Higgins (1968) and others (see references of Kasahara, 1976). The solutions are given by

$$(\tilde{u},\tilde{v},\tilde{h})^{\mathrm{T}} = \mathbf{S}_n\mathbf{H}_r^s(\lambda,\phi;\, n)\exp(-i\sigma_r^s t), \tag{5.1}$$

where the superscript T denotes the transpose, $\mathbf{S}_n$

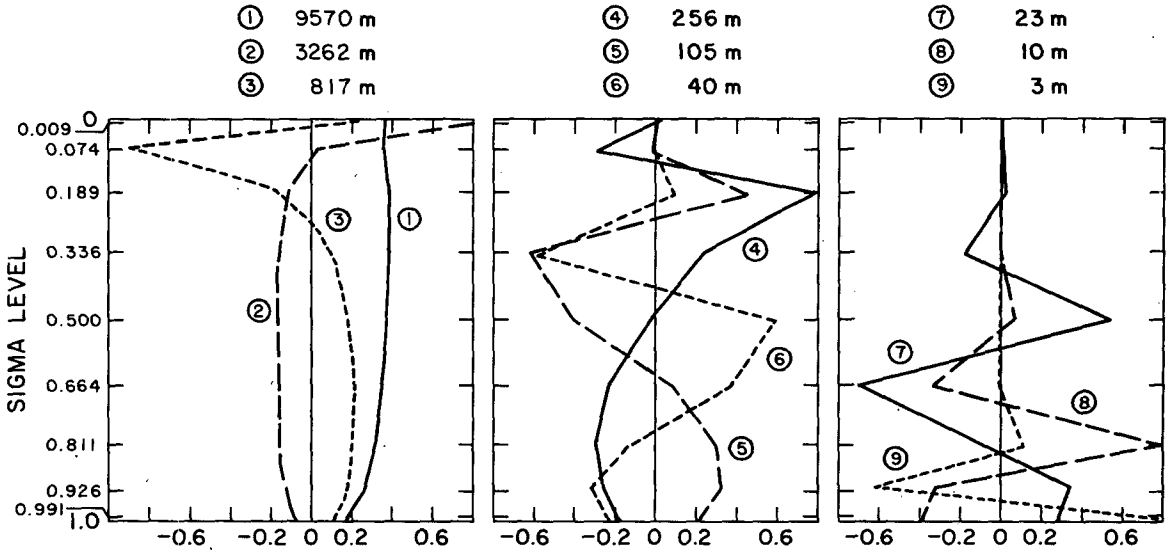

FIG. 2. Vertical profiles of eigenfunctions $\Phi_n(k)$ corresponding to equivalent heights D_n, the values of which are listed on the top.

is the scaling matrix

$$\mathbf{S}_n = \begin{pmatrix} (gD_n)^{1/2} & 0 & 0 \\ 0 & (gD_n)^{1/2} & 0 \\ 0 & 0 & D_n \end{pmatrix}, \quad (5.2)$$

D_n is the equivalent height and $\mathbf{H}_r^s(\lambda,\phi; n)$ are Hough harmonics (Kasahara, 1978) as functions of longitude λ and latitude ϕ corresponding to the nth vertical mode,

$$\mathbf{H}_r^s(\lambda,\phi; n) = \mathbf{H}_r^s(\phi; n)e^{is\lambda} \quad (5.3)$$

in which

$$\mathbf{H}_r^s(\phi; n) = \begin{pmatrix} U_r^s(\phi; n) \\ -iV_r^s(\phi; n) \\ Z_r^s(\phi; n) \end{pmatrix}. \quad (5.4)$$

The meridional structure function $\mathbf{H}_r^s$, called Hough vector function, and the eigenfrequency σ_r^s are dependent on three indices. One is zonal wavenumber s, another is meridional index r, and the third is vertical mode n.

Hough harmonics $\mathbf{H}_r^s$ are orthogonal in the sense that

$$\frac{1}{2\pi}\int_0^{2\pi}\int_{-1}^{1} \mathbf{H}_{r'}^{s'}\cdot(\mathbf{H}_r^s)^* d\mu d\lambda = \delta_{rr'}\delta_{ss'}, \quad (5.5)$$

where $\mu = \sin\phi$, the asterisk in (5.5) denotes the complex conjugate, and the dot denotes the inner product. This orthogonality is shown from the property of the linearized shallow-water equations (3.9)–(3.11) for $s \geq 1$. For $s = 0$, a degeneracy occurs for the modes corresponding to zero eigenfrequency and the orthogonality of these modes is undeterminable from the system of equations. However, it is possible to derive the set of orthogonal functions for these modes (Kasahara, 1978) and, therefore, the orthogonality condition is applicable to any integer s or s', $s \geq 0$ and $s' \geq 0$.

Two kinds of waves exist for the shallow-water equations (3.9)–(3.11)—high-frequency westward and eastward propagating inertia-gravity waves (the first kind) and low-frequency westward propagating rotational waves of Rossby-Haurwitz type (the second kind). Hough vector functions for different modes are denoted by different meridional indices—l_{EG}, l_{WG}, and l_R for eastward-propagating gravity-inertia waves (EG), westward-propagating gravity-inertia waves (WG) and rotational waves (R) for each zonal wavenumber s.

6. Energy relationships

Multiplying (3.1)–(3.4) by u', v', P' and $\partial P'/\partial\sigma$, respectively, and adding the resultant equations, we obtain

$$\frac{\partial}{\partial t}\left[\frac{1}{2}u'^2 + \frac{1}{2}v'^2 + \frac{1}{2}\frac{\sigma}{R\Gamma_0}\left(\frac{\partial P'}{\partial\sigma}\right)^2\right] = -\frac{\partial}{\partial\sigma}(P'W') - \nabla\cdot(P'\mathbf{V}').$$

Integration of the above equation globally with respect to longitude λ, latitude ϕ, and vertical coordinate σ and use of the boundary conditions (2.22) and (2.23) yields

$$\frac{\partial}{\partial t}\int_0^{2\pi}\int_{-1}^{1}\int_0^1 \left[\frac{1}{2}u'^2 + \frac{1}{2}v'^2 + \frac{1}{2}\frac{\sigma}{R\Gamma_0}\left(\frac{\partial P'}{\partial\sigma}\right)^2 + \frac{1}{2}\frac{1}{R(T_0)_H}P_H'^2\right]a^2 d\lambda d\mu d\sigma = 0, \quad (6.1)$$

where $\mu = \sin\phi$.

We express the variable u', v' and P' as the sum of n vertical modes

$$\left.\begin{aligned} u' &= \sum_n \tilde{u}_n\Psi_n(\sigma) \\ v' &= \sum_n \tilde{v}_n\Psi_n(\sigma) \\ P' &= \sum_n g\tilde{h}_n\Psi_n(\sigma) \end{aligned}\right\}. \quad (6.2)$$

Substitution of (6.2) into (6.1) yields

$$\frac{\partial}{\partial t}\int_0^{2\pi}\int_{-1}^{1}\int_0^1 \left\{\frac{1}{2}\left[\sum_n \tilde{u}_n\Psi_n\right]^2 + \frac{1}{2}\left[\sum_n \tilde{v}_n\Psi_n\right]^2 + \frac{1}{2}\frac{g^2\sigma}{R\Gamma_0}\left[\sum_n \tilde{h}_n\frac{d\Psi_n}{d\sigma}\right]^2 + \frac{1}{2}\frac{g^2}{R(T_0)_H}\left[\sum_n \tilde{h}_n(\Psi_n)_H\right]^2\right\} \times a^2 d\lambda d\mu d\sigma = 0. \quad (6.3)$$

The vertical structure function $\Psi_n(\sigma)$ satisfies the following equation

$$\frac{d}{d\sigma}\left(\frac{\sigma g}{R\Gamma_0}\frac{d\Psi_n}{d\sigma_i}\right) + \frac{1}{D_n}\Psi_n = 0 \quad (6.4)$$

according to (3.12). By multiplying (6.4) by Ψ_m, integrating the resulting equation with respect to σ from 0 to 1, and utilizing the boundary conditions in (3.13), we obtain

$$\int_0^1 \frac{\sigma g}{R\Gamma_0}\frac{d\Psi_m}{d\sigma}\frac{d\Psi_n}{d\sigma}d\sigma = \int_0^1 \frac{1}{D_n}\Psi_n\Psi_m d\sigma - \frac{g}{R(T_0)_H}(\Psi_m)_H(\Psi_n)_H.$$

Using the above relationship and the orthonormality condition (4.1) of Ψ_n, Eq. (6.3) reduces to

$$\frac{\partial}{\partial t}\int_0^{2\pi}\int_{-1}^{1}\sum_n \frac{1}{2}\left(\tilde{u}_n^2 + \tilde{v}_n^2 + \frac{g}{D_n}\tilde{h}_n^2\right)a^2 d\lambda d\mu = 0.$$

This demonstrates that the representation (6.2) in terms of the sum of n vertical modes permits the

partition of total energy into the kinetic and available potential energy of each vertical mode separately.

7. Expansion of three-dimensional data

Input data are given by

$$\left.\begin{aligned} u^{\mathrm{I}}[\lambda,\phi,\sigma(k)] &= u_{\mathrm{obs}} \\ v^{\mathrm{I}}[\lambda,\phi,\sigma(k)] &= v_{\mathrm{obs}} \\ P^{\mathrm{I}}[\lambda,\phi,\sigma(k)] &= gz_{\mathrm{obs}} + RT_0(\sigma)\ln p_H \end{aligned}\right\} . \quad (7.1)$$

The right-hand sides of (7.1) are given fields of velocity components and a combination of geopotential and surface pressure at location $[\lambda,\phi,\sigma(k)]$. The data in the vertical are placed at level k shown in Fig. 1 and hereafter index k will be used instead of $\sigma(k)$.

By defining the input data vector

$$\mathbf{X}^{\mathrm{I}}(\lambda,\phi,k) = (u^{\mathrm{I}},v^{\mathrm{I}},g^{-1}P^{\mathrm{I}})^{\mathrm{T}}, \quad (7.2)$$

we express projection of $\mathbf{X}^{\mathrm{I}}$ onto the vertical structure functions $\Phi_n(k)$ defined by (4.11),

$$\mathbf{X}^{\mathrm{I}}(\lambda,\phi,k) = \sum_{n=1}^{K} \mathbf{S}_n\mathbf{X}_n(\lambda,\phi)\Phi_n(k), \quad (7.3)$$

where $\mathbf{S}_n$ is the scaling matrix defined by (5.2).

Multiplying (7.3) by $\Phi_m(k)$, summing the result with respect to k from 1 to K, and utilizing the orthogonality condition (4.14), we obtain the vertical transform

$$\mathbf{X}_n(\lambda,\phi) = \mathbf{S}_n^{-1} \sum_{k=1}^{K} \mathbf{X}^{\mathrm{I}}(\lambda,\phi,k)\Phi_n(k). \quad (7.4)$$

The horizontal coefficient vector $\mathbf{X}_n(\lambda,\phi)$ for a given vertical mode n is now projected onto Hough harmonics as

$$\mathbf{X}_n(\lambda,\phi) = \sum_{r=1}^{R} \sum_{s=-M}^{M} X_r^s(n)\mathbf{H}_r^s(\lambda,\phi;n), \quad (7.5)$$

where zonal wavenumber s runs from a negative integer $-M$ to a positive integer M including zero. The summation for serial number r from 1 to R include three meridional modes, l_{EG}, l_{WG} and l_{R}.

To obtain the scalar coefficient $X_r^s(n)$, we multiply (7.5) by $[\mathbf{H}_l^m]^*$, integrate the resultant equation with respect to λ from 0 to 2π and ϕ from $-\pi/2$ to $\pi/2$, and utilize the orthonormality condition (5.5). The result is

$$X_r^s(n) = \frac{1}{2\pi}\int_0^{2\pi}\int_{-1}^{1} \mathbf{X}_n(\lambda,\phi)\cdot[\mathbf{H}_r^s]^* d\mu d\lambda, \quad (7.6)$$

where $\mu = \sin\phi$. The integral on the right-hand side can be split into the two transforms by using the definition of $\mathbf{H}_r^s$ given by (5.3):

$$X_r^s(n) = \int_{-1}^{1} \mathbf{Y}(\phi;n)\cdot[\mathbf{H}_r^s]^* d\mu, \quad (7.7)$$

$$\mathbf{Y}(\phi;n) = \frac{1}{2\pi}\int_0^{2\pi} \mathbf{X}_n(\lambda,\phi)e^{-is\lambda}d\lambda. \quad (7.8)$$

Formula (7.7) is the Hough transform and the integration can be performed by the Gaussian quadrature. Formula (7.8) is the Fourier transform and a fast Fourier transform routine is available for calculation of the integral.

8. Results

We present results of spectral analysis on the Northern Hemisphere NMC Flattery daily data for the month of January 1977. We assume the data to be symmetric with respect to the equator in dealing with the Northern Hemisphere alone. Hence, we used only symmetric Hough vector functions which are symmetric for the zonal wind component and the geopotential and antisymmetric for the meridional wind component. The NMC data which are available on a 2.5° longitude and latitude grid were interpolated to a grid consisting of 96 longitudes and 40 Gaussian latitudes from the North Pole to the equator. The data on this latter grid were then interpolated to the nine sigma levels as shown on the left-hand side of Fig. 2.

We constructed Hough harmonics $\mathbf{H}_r^s$ defined by (5.3) for $0 \leq |s| \leq 18$ with seven vertical modes corresponding to the equivalent heights of 9570, 3262, 817, 256, 105, 40 and 23 m as shown in Fig. 2. The method of computation is described in Kasahara (1976, 1978). For $|s| > 0$, we used 20 symmetric modes ($l_{\mathrm{EG}} = 0, 2, 4, 6$; $l_{\mathrm{WG}} = 0, 2, 4, 6$; $l_{\mathrm{R}} = 1, 3, 5 \ldots, 23$) of Hough vector functions. For $s = 0$, we adopted Hough vector functions consisting of 11 gravity-inertia modes ($l_{\mathrm{WG}} = 0, 2, 4, \ldots, 20$) and 19 geostrophic modes ($l_{\mathrm{R}} = 1, 3, 5, \ldots, 37$). For gravity-inertia modes for $s = 0$, we need to store only those of either positive or negative frequency, because Hough vector functions of positive and negative frequencies are in complex conjugate and this property can be taken into account in the expansion.

The coefficients $X_r^s(n)$, defined by (7.6), are calculated for the month of January 1977 on a daily basis except for 15 January which was missing from the source tapes archived at NCAR. Since the expansion coefficients $X_r^s(n)$ are common to both the mass and wind fields and are dimensionless, we must multiply the coefficients by D_n or $(gD_n)^{1/2}$ to express them with proper units of height (m) or speed (m s^{-1}) for geopotential height or wind, respectively. Also, the expansion coefficients are complex so that their magnitudes are calculated by

$$|X_r^s(n)| = \{\mathrm{Re}[X_r^s(n)]^2 + \mathrm{Im}[X_r^s(n)]^2\}^{1/2},$$

where Re and Im denote the real and imaginary parts, respectively.

To present results through familiar physical units, we will show the spectra of total energy in terms of kinetic energy in units of $m^2\ s^{-2}$ by multiplying $|X_r^s(n)|^2$ by gD_n after taking their arithmetic mean for 30 days.

Fig. 3 shows the total kinetic energy contained in all zonal wavenumbers s from 1 to 18 and all species of waves for each vertical mode n calculated from

$$\sum_{r=1}^{20}\sum_{s=1}^{18} gD_n|X_r^s(n)|^2.$$

The sum with respect to meridional index r includes all meridional components of rotational and gravity-inertia modes used. As demonstrated in Section 6, the present decomposition enables us to compare kinetic energies in various vertical modes. As expected, the total energy is largest for the external mode ($n = 1$) and then decreases, in general, as the function of vertical mode n, except for the second internal mode ($n = 3$) which contains only a small amount of kinetic energy. However, the vertical modes $n = 4$ and 5 still contain substantial amounts of energy. As seen from Fig. 2, the $n = 3$ mode has a large weight in the stratosphere. The present analysis indicates that the motions corresponding to this type of mode are very weak. Whether this particular result is a characteristic of the set of data used or not remains to be investigated further.

From the work of Obukhov (1960), Holmström (1963), and Bradley and Wiin-Nielsen (1968), it is generally recognized that a large percentage of kinetic energy is contained in the gravest vertical mode, namely, the external mode, and the percentages of energy contained in other vertical modes are relatively small. Although the present result agrees qualitatively with this observation, the amount of kinetic energy contained in the higher vertical modes in the present analysis is much larger than that in the earlier studies. This difference may be expected, because these earlier results on the vertical structure of atmospheric motions were based on the empirical orthogonal function expansion which is efficient in the representation of data, but the vertical structure functions thus obtained do not have a well-defined physical significance. On the other hand, the normal mode expansion is not an efficient means to represent data from the viewpoint of best fit, but the procedure has the advantage of interpreting the vertical modes physically. It is important to note, however, that the basic state selected for the construction of the normal mode functions is an atmosphere at rest, though the mean temperature T_0 varies in height.

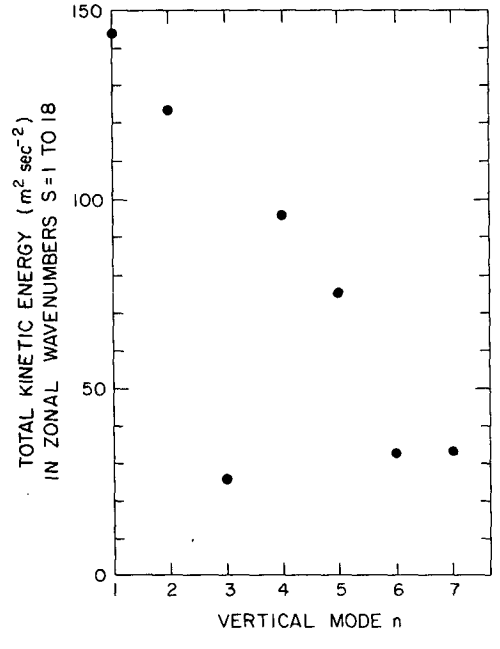

FIG. 3. Total kinetic energy contained in all zonal wavenumbers $s = 1$ to 18 is plotted against vertical mode n.

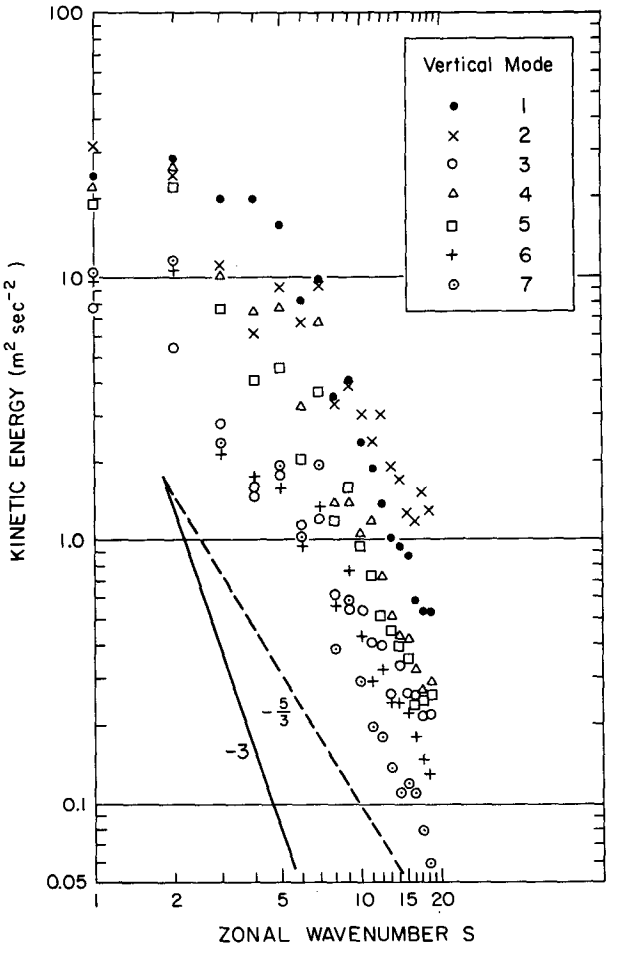

FIG. 4. Partial kinetic energy contained in each vertical mode n is plotted against zonal wavenumber s.

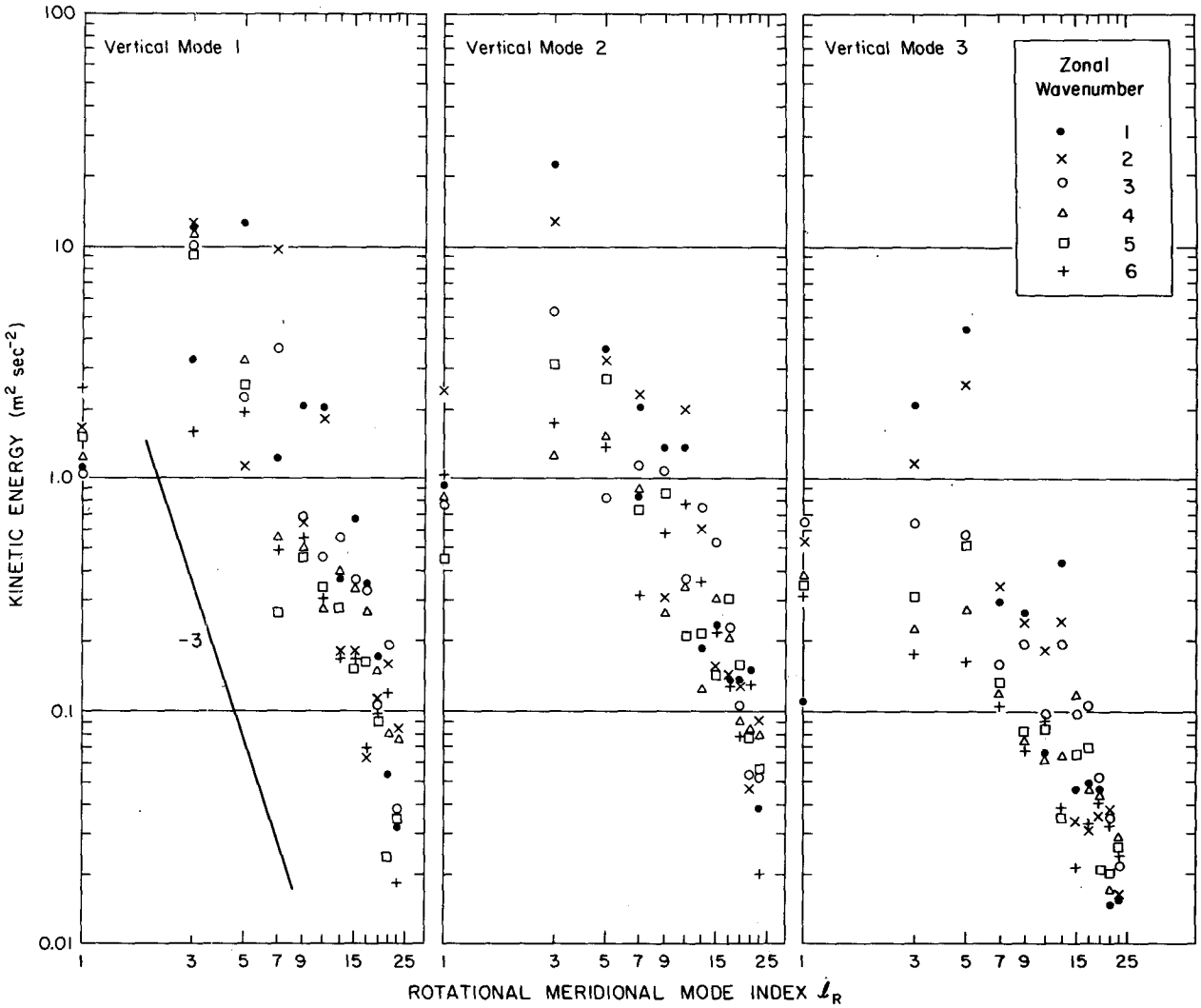

FIG. 5a. Plot of specific kinetic energy for each vertical mode $n = 1$ to 3, rotational meridional index l_R, and zonal wavenumber $s = 1$ to 6.

Hence, the present vertical structure functions are expected to be different from those constructed on the atmospheric basic state which include mean motions. Also, there is a tendency that percentage-wise more energy is partitioned into the external mode if the model top is placed at a relatively low altitude such as the 200 mb level. The influence of model top height on the energy partition should be investigated in the future.

Fig. 4 shows the partial kinetic energy contained in each zonal wavenumber s and in each vertical mode n calculated from

$$\sum_{r=1}^{20} gD_n|X_r^s(n)|^2.$$

The solid line denotes the slope of s^{-3} and the dashed line the slope of $s^{-5/3}$. The energy spectra for planetary waves of wavenumber $s > 8$ seem to satisfy the -3 power law (Leith, 1971) for each vertical mode, except for the mode $n = 2$ and 3 whose spectrum, respectively, is closer to the $-5/3$ power law.

Figs. 5a and 5b show the plot of specific kinetic energy $gD_n|X_r^s(n)|^2$ for vertical mode $n = 1$ to 6, rotational meridional index $l_R = 1, 3, \ldots, 23$, and zonal wavenumber $s = 1$ to 6. The left-hand panel of Fig. 5a is for vertical mode $n = 1$, the external mode. The spectral peaks generally appear around meridional index $l_R = 3 \sim 7$ and then energy decreases sharply following approximately a -3 power slope. This tendency is observed in each vertical mode up to $n = 4$ in Fig. 5b. For vertical modes $n = 5$ and 6, the spectral peaks for low zonal wavenumbers shift toward a higher meridional index $l_R = 7 \sim 11$ for $n = 5$ and $l_R = 11 \sim 23$ for $n = 6$. For vertical modes $n = 5$ and 6, the amount of

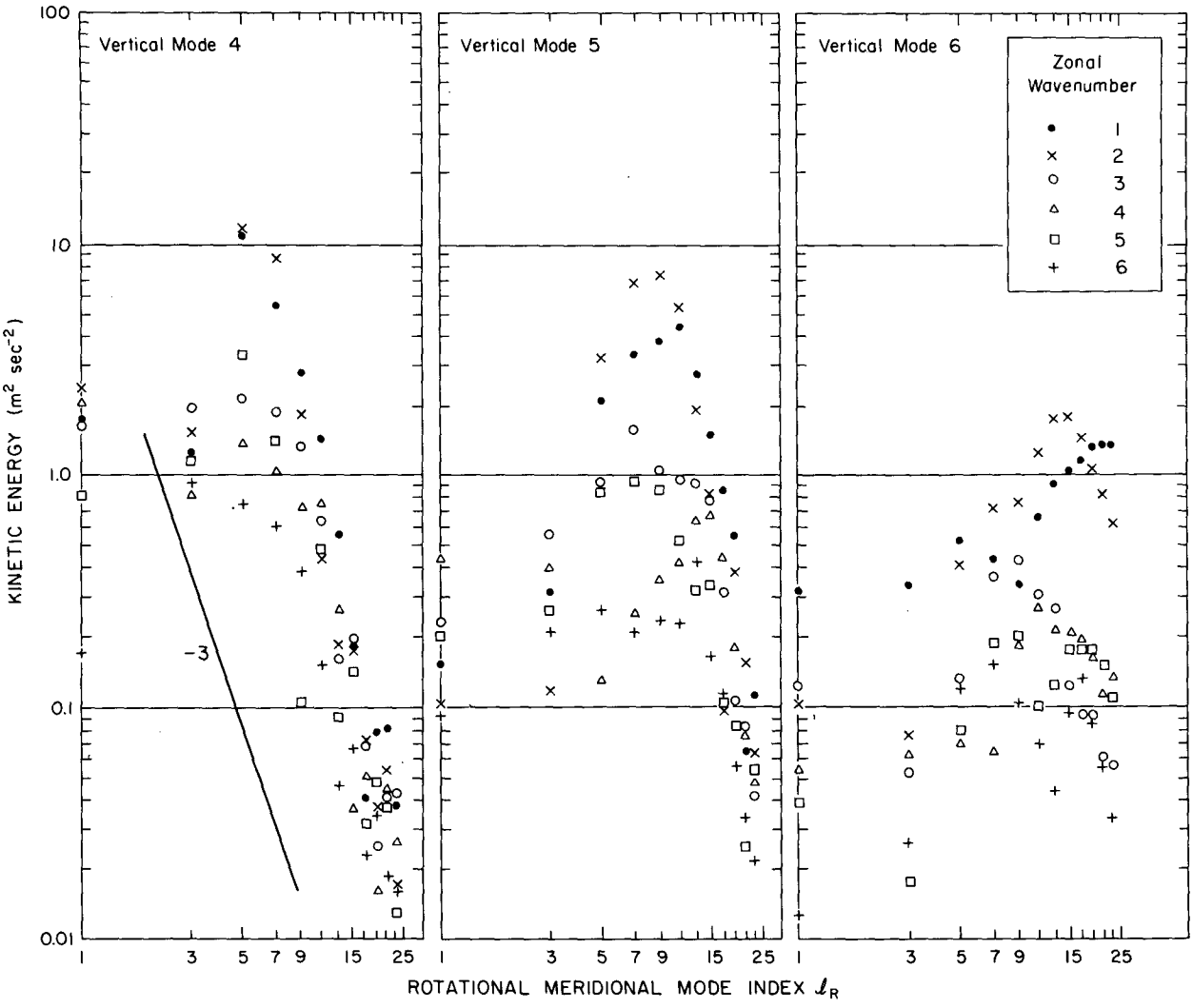

FIG. 5b. As in Fig. 5a except for vertical mode n = 4 to 6.

energy becomes smaller and the spectral distribution flatter for higher zonal wavenumbers s. These features seem to be characteristic of the higher vertical modes.

Fig. 6 shows the spectral distributions of specific kinetic energy with respect to zonal wavenumber s for westward propagating gravity-inertia mode $l_{WG} = 0$ (left panel) and eastward propagating Kelvin mode $l_{EG} = 0$ (right panel). As expected, their magnitudes are considerably smaller than those of the rotational modes. (Note the scale of energy on the left ordinate.) Their magnitudes are comparatively large in low zonal wavenumbers and decrease toward higher zonal wavenumbers. Their magnitudes are large for the vertical mode $n = 1$ and 2 in particular and become smaller in higher vertical modes. The energy spectra of other gravity-inertia modes ($l_{EG} = 2, 4, 6$, and $l_{WG} = 2, 4, 6$) exhibit generally the same features, though their magnitudes are smaller. Those results are not shown here, because we are not certain that the magnitudes of the gravity-inertia modes in the present data are representative. As we mentioned earlier, the present data are based on the Flattery analysis. Hence the results may be biased by the fact that only the rotational components of Hough harmonics corresponding to the external mode were employed in the analysis procedure (Flattery, 1970).

The left panel of Fig. 7 shows the spectral distributions of specific kinetic energy with respect to geostrophic meridional index l_R for zonal wavenumber $s = 0$, the zonal mean component. The low geostrophic modes are about one to two orders of magnitude larger than the rotational modes of wave components ($s > 0$). Their magnitudes decrease generally toward higher geostrophic meridional indices with the rate of decrease even higher than a -3 power slope. Because of this steeper rate of

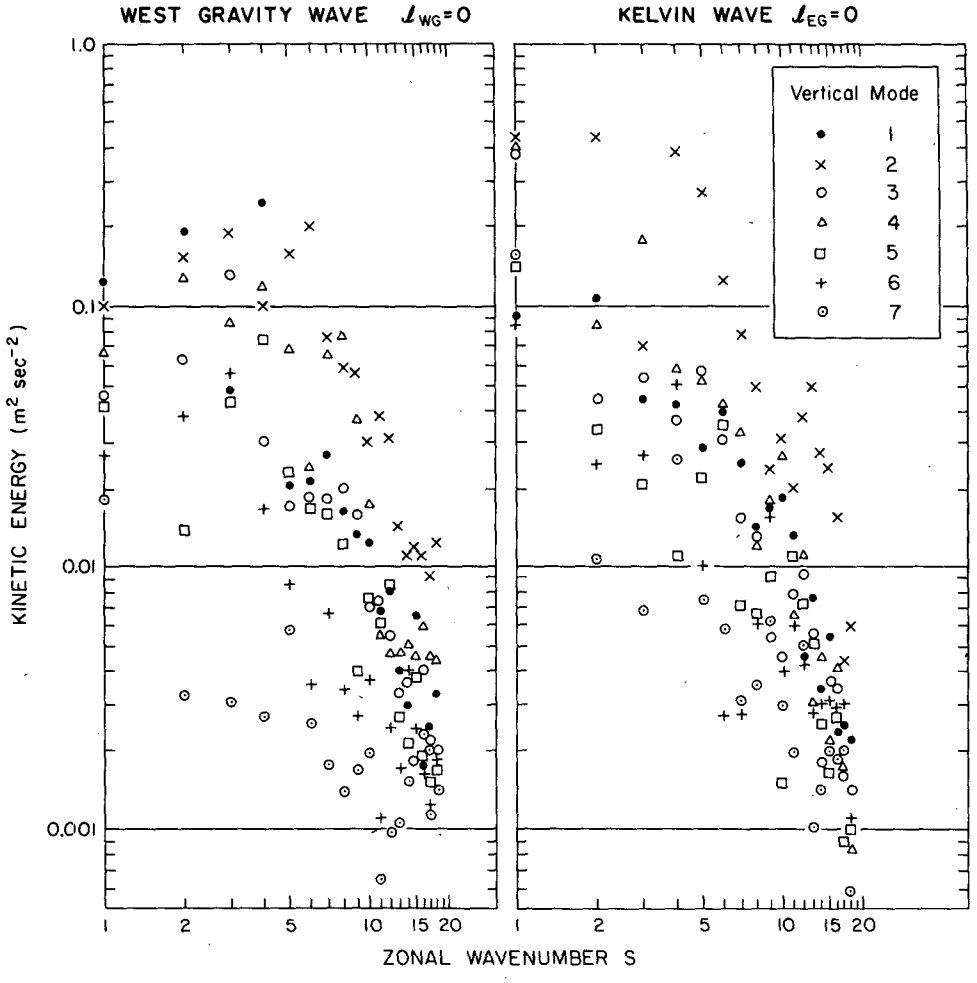

FIG. 6. Spectral distributions of partial kinetic energy with respect to zonal wavenumber s and vertical mode n for westward propagating gravity-inertia wave $l_{WG} = 0$ (left panel) and eastward propagating Kelvin wave $l_{EG} = 0$ (right panel).

decrease, the energy level of 0.01 m^2 s^{-2} can be reached at about $l_R = 25$. This means, by comparing with Fig. 5a, that the expansion of zonal mean fields in terms of geostrophic meridional modes requires no more terms than those required for the expansion of nonzonal fields in terms of rotational models.

The right panel of Fig. 7 shows the spectral distributions of specific kinetic energy with respect to gravity-inertia mode l_G for zonal wavenumber $s = 0$. Their magnitudes are about one order larger than the order of magnitudes of gravity-inertia modes for nonzonal components ($s > 0$). For the representation of zonally-averaged fields ($s = 0$), the role of gravity-inertia components is substantial, because the zonally-averaged meridional velocity component is represented only by gravity-inertia components. Although the magnitudes of gravity-inertia modes generally decrease toward higher meridional indices, the distribution tends to scatter for the vertical mode $n = 2$.

Fig. 8 shows schematically a maximum horizontal resolution range in zonal wavenumber s and rotational meridional index l_R for each vertical mode n. The domains inside of the solid lines denote the regions in which specific kinetic energy $gD_n|X_r^s(n)|^2$ is larger than 0.1 m^2 s^{-2}. The numerals on the solid lines indicate vertical mode n. Since the calculations were performed with the maximum $s = 18$ and the maximum $l_R = 23$, the lines extending outside of the computational resolution are estimated by extrapolation and distinguished by dashed lines. From this figure it appears that more vertical modes are needed to represent data in the ultralong wave regions as further discussed in the next section.

9. Conclusions

We presented the construction of three-dimensional NMF's based on a global primitive equation model to represent the wind and mass fields simultaneously. In contrast to the combination of the

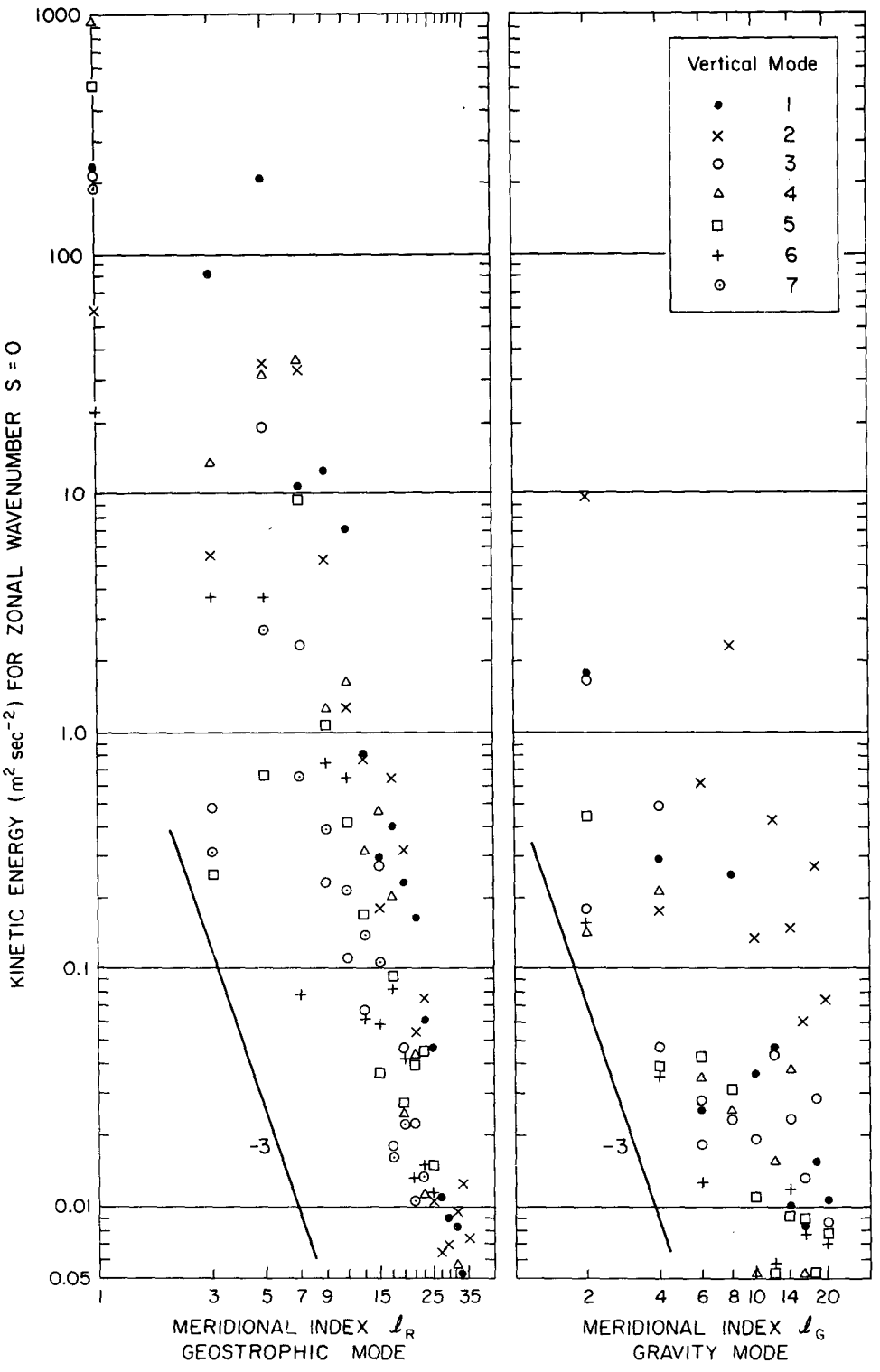

FIG. 7. Spectral distributions of specific kinetic energy for zonal wavenumber $s = 0$ and vertical modes $n = 1$–7 with respect to geostrophic meridional index l_R (left panel) and gravity-inertia meridional index l_G (right panel).

empirical orthogonal function expansion in the vertical and the spherical harmonic expansion in the horizontal, the present method enables us to examine the partition of energy into two distinct kinds of motions—gravity-inertia modes and rotational modes of Rossby/Haurwitz type. Both kinds of mo-

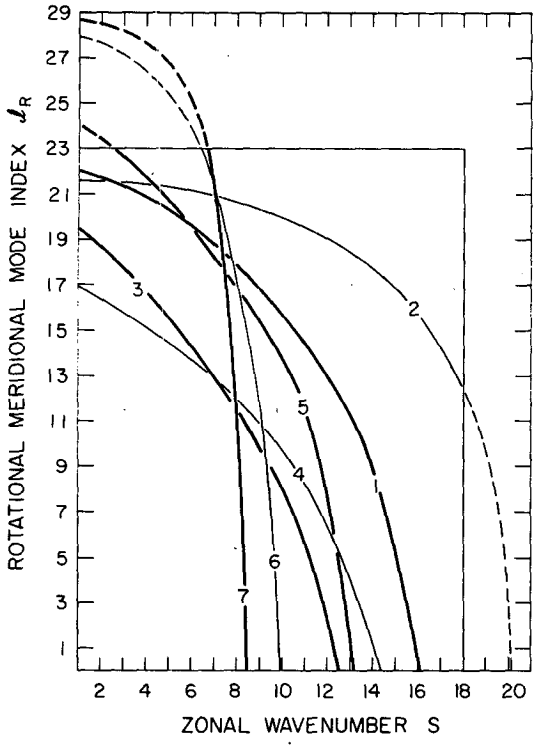

FIG. 8. A maximum horizontal resolution range in zonal wavenumber s and rotational meridional index l_R for each vertical mode n. The numerals on the solid lines indicate vertical mode n. The domains inside the solid lines denote the regions in which specific kinetic energy $gD_n|X_l^s(n)|^2$ is larger than 0.1 m^2 s^{-2}.

tions are also partitioned into different vertical modes. The gravest vertical mode is referred to as external and the remaining vertical modes as internal.

We applied the spectral analysis to the Northern Hemisphere NMC data for the month of January 1977. We found that the external mode contains the largest amount of energy, but internal modes, particularly vertical modes $n = 2, 4, 5$, contain relatively large energy. The vertical structure functions depend on the location and number of levels in the vertical where data are placed and the profile of the static stability. The possibility of placing the data levels in the vertical in such a way that the amount of energy contained in the internal modes decreases with respect to vertical mode n faster than shown in Fig. 3 should be further investigated.

In each vertical mode, partial kinetic energy contained in all meridional indices tends to decrease as functions of zonal wavenumber s following a -3 power law as shown in Fig. 4. This result is consistent with the past studies on spectral energy distribution discussed in the Introduction (e.g., Leith, 1971; Baer, 1972, 1981).

In lower vertical modes ($n = 1 \sim 4$), energy tends to distribute uniformly in zonal wavenumber s and rotational meridional index l_R. For a given zonal wavenumber, energy tends to decrease as the function of l_R following a -3 power law too. On the other hand, in higher vertical modes ($n = 5 \sim 7$), energy tends to distribute *nonuniformly* concentrating in lower s and higher l_R. In other words, in lower vertical modes the energy distribution may be represented by the triangular-type truncation in (s,l_R) domain, while in higher vertical modes the energy distribution is represented more preferably by a parallelogramic truncation in (s,l_R) domain. Daley and Bourassa (1978) investigated the question as to which of the two truncations, rhomboidal or triangular, in a spherical harmonic spectral primitive equation model is superior for real data forecasting. They found that the two truncation methods produced forecasts of equivalent accuracy. The present result indicates that the question of horizontal truncation in a spectral model may be related to which vertical mode we are concerned with.

An important implication of Fig. 8 is that we need more vertical modes to represent data in the ultralong wave region. Moreover, these internal modes require higher latitudinal modes to represent. Although the latter finding seems to be surprising at first, this is indeed the case of large-scale motions in the stratosphere for which we need only a few degrees of freedom in the longitudinal direction, yet a relatively large number of resolutions is required to represent their latitudinal variations.

The observational finding that more vertical modes are required to represent satisfactorily long planetary waves is not inconsistent with a theoretical deduction by Nakamura (1976) that to represent stationary long planetary waves correctly one requires vertical resolutions of 1–2 km grid increment in the troposphere and 2–3 km grid increment in the stratosphere. We do not gain forecast accuracies of large-scale motions by merely increasing the horizontal grid resolution without correspondingly improving the vertical grid resolution of a prediction model.

With respect to the spectral distribution of energy for zonally-averaged flow, i.e., zonal wavenumber $s = 0$ (Fig. 7), we found that the expansion of zonal mean fields in terms of geostrophic modes requires no more terms than those required for the expansion of nonzonal fields in terms of rotational modes. Moreover, a comparison between the left-hand panel of Fig. 5a and that of Fig. 7 suggests that the number of vertical modes required to represent the zonal mean fields is no more than that required to represent the nonzonal fields.

In general, energy of gravity-inertia waves is very small compared with that of rotational waves and appears to concentrate mostly in the first internal mode ($n = 2$). This result, however, may not be representative due to the fact that the present data are biased toward giving smaller amplitudes of gravity-inertia waves in the Flattery analysis pro-

cedure. We plan to repeat the computation using the NMC multivariate analysis daily data to evaluate the magnitudes of gravity-inertia modes in the atmosphere.

Finally, it is remarked that the representation of data in terms of three-dimensional NMF's has a definite advantage in application to the objective analysis of meteorological data in which an initialization scheme to a primitive equation model is automatically incorporated. The discussion, however, is outside of the scope of the present work.

Acknowledgments. The authors thank R. Daley, J. Tribbia and D. Williamson for discussions and useful comments on this work. The manuscript was typed by Mary Niemczewski. Drafting of the figures was performed by the NCAR Graphics Department.

REFERENCES

Baer, F., 1972: An alternate scale representation of atmospheric energy spectra. *J. Atmos. Sci.*, **29**, 649–664.

——, 1981: Three-dimensional scaling and structure of atmospheric energetics. *J. Atmos. Sci.*, **38** (in press).

Bourke, W., B. McAvaney, K. Puri and R. Thurling, 1977: Global modeling of atmospheric flow by spectral methods. *Methods Comput. Phys.*, **17**, 268–324.

Bradley, J. H. S., and A. Wiin-Nielsen, 1968: On the transient part of the atmospheric planetary waves. *Tellus*, **20**, 533–544.

Burrows, W. R., 1976: A diagnostic study of atmospheric spectral kinetic energetics. *J. Atmos. Sci.*, **33**, 2308–2321.

Chen, T.-C., and A. Wiin-Nielsen, 1978: On nonlinear cascades of atmospheric energy and enstrophy in a two-dimensional spectral index. *Tellus*, **30**, 313–322.

Daley, R., 1979: The application of nonlinear normal mode initialization to an operational forecast model. *Atmosphere-Ocean*, **17**, 97–124.

——, and Y. Bourassa, 1978: Rhomboidal versus triangular spherical harmonic truncation: some verification statistics. *Atmosphere-Ocean*, **16**, 187–196.

Flattery, T., 1970: Spectral models for global analysis and forecasting. *Proc. Sixth AWS Technical Exchange Conference*, U.S. Naval Academy, Air Weather Service Tech. Rep. 242, 42–54.

Gavrilin, B. L., 1965: On the description of vertical structure of synoptical processes. *Izv. Atmos. Ocean. Phys.* **1**, 8–17.

Holmström, I., 1963: On a method for parametric representation of the state of the atmosphere. *Tellus*, **15**, 127–149.

——, 1964: On the vertical structure of the atmosphere. *Tellus*, **16**, 1–22.

Kasahara, A., 1976: Normal modes of ultralong waves in the atmosphere. *Mon. Wea. Rev.*, **104**, 669–690.

——, 1978: Further studies on a spectral model of the global barotropic primitive equations with Hough harmonic expansions. *J. Atmos. Sci.*, **35**, 2043–2051.

Leith, C. E., 1971: Atmospheric predictability and two-dimensional turbulence. *J. Atmos. Sci.*, **28**, 145–161.

Longuet-Higgins, M. S., 1968: The eigenfunctions of Laplace's tidal equations over a sphere. *Phil. Trans. Roy. Soc. London*, **A262**, 511–607.

Nakamura, H., 1976: Some problems in reproducing planetary waves by numerical models of the atmosphere. *J. Meteor. Soc. Japan*, Ser. II, **54**, 129–146.

Obukhov, A. M., 1960: The statistically orthogonal expansion of empirical functions. *Izv. Geophys. Ser.*, No. 3, 288–291.

Robert, A., J. Henderson and C. Turnbull, 1972: An implicit time integration scheme for baroclinic models of the atmosphere. *Mon. Wea. Rev.*, **100**, 329–335.

Temperton, C., and D. L. Williamson, 1979: Normal mode initialization for a multi-level gridpoint model. Tech. Rep. No. 11, European Centre for Medium Range Weather Forecasts, Shinfield Park, Reading, England, 91 pp.

Wiin-Nielsen, A., 1971: On the motion of vertical modes of transient, very long waves. Part I. Beta plane approximation. *Tellus*, **23**, 87–98.

Williamson, D. L., and R. E. Dickinson, 1976: Free oscillations of the NCAR global circulation model. *Mon. Wea. Rev.*, **104**, 1372–1391.